Density Functional Theory Studies of the Interaction of H, S, Ni−H, and Ni−S Complexes with the MoS_2 Basal Plane

Dan C. Sorescu,*,†,‡ David S. Sholl,†,§ and Anthony V. Cugini†

U.S. Department of Energy, National Energy Technology Laboratory, P.O. Box 10940, Pittsburgh, Pennsylvania 15236, Department of Chemical and Petroleum Engineering, University of Pittsburgh, Pittsburgh, Pennsylvania 15261, and Department of Chemical Engineering, Carnegie Mellon University, Pittsburgh, Pennsylvania 15213

Received: June 26, 2003; In Final Form: October 23, 2003

First principles calculations based on spin-polarized density functional theory and the generalized gradient approximation have been used to study the interaction of atomic and molecular hydrogen and sulfur species with bare and Ni modified MoS_2(0001). The calculations employ slab geometries and periodic boundary conditions. Our calculations indicate that H_2 can be adsorbed on this surface only when sulfur defect sites are present. In this case a dissociative chemisorption process with an activation barrier of about 22 kcal/mol has been identified. Adsorption of atomic hydrogen is possible on the nondefective surface with binding energies in the range 8−16 kcal/mol. On the sulfur defective surface, the binding energy of atomic hydrogen increases to 62.2 kcal/mol. Similarly, S atoms can adsorb on the bare surface with adsorption energies in the range 33−42 kcal/mol depending on the surface coverage. For the surface with preadsorbed Ni atoms, these atoms can serve as adsorption centers for both H_x and S_x ($x = 1,2$) species. Additionally, they can assist dissociation of H_2 molecules. As a result of hydrogenation or sulfiding, the interaction of Ni adatoms with the surface decreases by as much as 50% relative to the case of bare Ni atoms. In turn, this leads to a decrease of the diffusion barriers of Ni−H and Ni−S_x ($x = 1,2$) complexes relative to the case of bare Ni atoms.

I. Introduction

Understanding the fundamental catalytic interactions that take place on various metal−sulfide catalysts such as molybdenum disulfide (MoS_2) represents an area of active research because such materials are promising candidates for production of clean fuels by hydrotreating and hydrodesulfurization (HDS) processes in petroleum-refining industries.[1,2] In practical applications, well-dispersed MoS_2 nanocrystallites supported on γ-alumina are used in either nonpromoted or promoted forms. In the case of nonpromoted systems, the main catalytic activity is provided at the edges of the MoS_2 clusters where sulfur vacancies are created.[3] Substantial increases in the performance of the MoS_2 catalysts can be obtained however by the aid of metallic promoters such as Co or Ni. For such systems, it is generally accepted that Co−Mo−S and Ni−Mo−S structures consisting of small MoS_2 clusters with promoter atoms located at the edges, are responsible for the HDS activity.[1,4,5]

However, precise identification of the location of the promoter species as well as their role upon the reactivity still continues to be a subject of intense investigations. For instance, the real-space atomic structure of promoted MoS_2 surfaces has recently been revealed using surface science techniques. Based on STM investigations, Besenbacher and co-workers[6] have shown that, at 400 K and in a H_2S atmosphere of 1×10^{-6} mbar, supported MoS_2 nanoclusters are triangular. This shape changes in the presence of Co promoter atoms from triangular to hexagonally truncated.[7] In this case, the Co atoms were found to be located preferentially at the $(\bar{1}010)$S-edges of the Co−Mo−S nanoclusters where they substitute into Mo positions. In the case of nonpromoted MoS_2 surfaces, recent STM and density functional theory (DFT) calculations have indicated that catalytic activity can be associated with one-dimensional metallic states located at the edge states of the MoS_2 nanocrystals.[8]

In a related series of papers from Toulhoat and co-workers,[9−13] the structural, energetic, and electronic properties of the$(10\bar{1}0)$and $(\bar{1}010)$edge-promoted MoS_2 catalysts have been characterized based on DFT calculations. Additionally, various intercalation and pseudointercalation configurations have been identified in which the promoter atoms interact with MoS_2 basal plane inside the van der Waals gap.[12] It was found that the most favorable configuration corresponds to a tetrahedral pseudo-intercalated position where the promoter is 4-fold coordinated by sulfur atoms and has one molybdenum neighbor. Another important finding of these studies was that the concentration of active sites as well as the shape of the MoS_2 crystallite depend significantly on the temperature and pressure conditions used in practical HDS processes. For example, it has been demonstrated[13] that the chemical potential of S, which depends on temperature and the pressure ratio of H_2S and H_2 species, has a direct influence on the shape of the MoS_2 crystallite and the local edge structure. A high chemical potential of sulfur leads to triangular-shaped particles terminated by the Mo-edge surface, in qualitatively good agreement with experimental STM images of Helveg et al.[6] Similar work performed by Schweiger et al.[14] has revealed, based on combined DFT and thermodynamics calculations, that the morphology of Co(Ni)/MoS nanocatalysts is directly dependent on sulfo-reductive conditions used in hydrotreatment processes and is promoter sensitive.

Investigation of the interactions of metallic promoters with the basal plane of MoS_2 has received less attention, as this surface is known to be catalytically inactive.[15] Nonetheless, there

* To whom correspondence should be addressed.
† National Energy Technology Laboratory.
‡ University of Pittsburgh.
§ Carnegie Mellon University.

10.1021/jp035824s CCC: $27.50
Published on Web 12/09/2003

are a variety of interesting issues regarding these interactions that remain unresolved. There have been several experimental studies from Weiss and co-workers[16−18] in which the dynamics of Ni and Co promoted MoS_2 basal planes was analyzed with atomic resolution. Low-temperature scanning tunneling microscopy images have indicated the presence of surface species that have a low barrier for diffusion. At temperatures as low as 4 K, Ni clusters ranging in size from a few atoms to larger islands were observed. It was suggested that these promoters could be used to increase the sticking probability of sulfur-containing hydrocarbons and to transport these hydrocarbons to the active sites for reaction. In addition, Weiss's experiments suggest that an important role in chemisorption of promoter species can be played by sulfur defects seen in STM images. Several questions raised by these experiments still have not been fully answered. For example, the location of the promoters on the basal plane or the electronic modifications induced upon adsorption of these metallic atoms was not well established. Moreover, the transport properties, particularly the diffusion and clustering characteristics of these promoters on MoS_2 have not been yet been fully characterized.

A first step to describe the interaction of Ni atoms with MoS_2 basal planes theoretically was made by Rodriguez.[19] Using INDO/S and unrestricted Hartree−Fock calculations in conjunction with cluster models representing $MoS_2(0001)$ and $MoS_2(10\bar{1}0)$ surfaces, it was determined that a significant reduction (0.5−2 eV) in the stability of the HOMOs takes place upon Ni adsorption. On the basal plane, it was found that H_2 and thiophene molecules are only weakly bound but the binding energy is increased when Ni atoms are present on the surface. These results suggest that one role played by Ni atoms when adsorbed on basal MoS_2 surface is to enhance the chemical activity of this surface by providing sites for chemisorption of thiophene.

In a recent study,[20] we used spin-polarized DFT calculations to investigate the chemisorption and diffusion properties of Ni atoms and clusters and a Ni−thiophene complex on the defect-free $MoS_2(0001)$ surface. We have identified several adsorption configurations of Ni atoms on the surface. The most stable configuration corresponds to adsorption at 3-fold hollow sites. Minimum energy pathways for the diffusion of Ni atoms between various local minima indicate the existence of relatively large barriers for hopping with values between 20 and 44 kcal/mol. We have also found that Ni atoms significantly increase the adsorption energy and the residence time of the thiophene molecule on the surface. However, the activation energy for diffusion of the Ni−thiophene complex is high, with a value of 21.2 kcal/mol. This result indicates that for temperatures below room-temperature, individual Ni atoms cannot transport thiophene molecule on the surface as suggested by Weiss et al.[17] One of the main results of our previous work is that the diffusion barriers that exist for isolated Ni atoms and small Ni clusters on $MoS_2(0001)$ are much larger than the apparent barriers of the surface species observed experimentally to diffuse rapidly on this surface. In the same study,[20] we suggested that a possible mechanism to decrease the diffusion barrier of Ni atoms on MoS_2 basal plane is by decorating the metallic atoms with H or S atoms that can be abstracted from the surface or from contaminants in the experimental system. In the present study, we investigate these aspects by examining, based on DFT calculations, the adsorption and diffusion properties of Ni−X (X = H, H_2, S, S_2, SH, H_2S) complexes on the defect-free MoS_2 basal plane. As in our previous study the periodic nature of the surface has been considered here by using a tridimensional slab model (supercell model) repeated periodically in all three directions. Besides providing a description of the geometric and energetic properties of Ni atoms and clusters adsorbed at various sites on $MoS_2(0001)$ surface, we also report the adsorption properties of H, H_2, and S species on both nondefective and defective surfaces. We emphasize that as in the case of our previous study[20] the main aim of our work is to examine the fundamental mechanisms of adsorption and diffusion for Ni−H and Ni−S species on the MoS_2 basal plane without including the full range of surface species and catalytically active edge sites that exist under the conditions necessary for practical HDS catalysts.

The organization of the paper is as follows. Section II describes our computational methods. The results of total energy calculations for adsorption of H_x, S_x, and Ni−H_xS_y ($x,y = 1,2$) complexes as well as a description of the minimum energy pathways between different equilibrium configurations are given in section III. We summarize the main conclusions in section IV.

II. Computational Methods

The first-principles calculations reported in this study were done using the same method as described in our previous work.[20] We have used the first principles total-energy program VASP (Vienna ab initio simulation program) and the ultrasoft pseudopotential database contained therein.[21−23] This program evaluates the total energy of periodically repeating geometries based on density-functional theory and the pseudopotential approximation. In this case, the electron−ion interaction is described by fully nonlocal optimized ultrasoft pseudopotentials (USPs) similar to those introduced by Vanderbilt.[24,25] All calculations have been done using the spin polarized PW91 generalized gradient approximation (GGA) of Perdew et al.[26] Periodic boundary conditions are used, with the one electron pseudo-orbitals expanded over a plane wave basis set. The expansion includes all plane waves whose kinetic energy is less than a cutoff energy of 242 eV. Optimization of different atomic configurations was based upon a conjugate-gradient minimization of the total energy, using the Hellmann−Feynman forces on the atoms. The results obtained using ultrasoft pseudopotentials were also checked in a few instances based on the projector augmented wave (PAW) method.[27,28]

Minimum energy paths between different minima were optimized by use of the nudged elastic band (NEB) method of Jónsson and co-workers.[29] In the NEB searches, between 8 and 16 images were employed between minima.

The surface model used in this study is the same as the one we used previously to characterize the chemisorption and diffusion properties of Ni atoms:[20] a surface supercell containing 3×3 surface units with one S−Mo−S trilayer. This model contains 9 Mo and 18 S atoms. A vacuum width of about 11 Å was used to separate neighbor slabs.

In our previous study,[20] we detailed the tests performed to benchmark the accuracy of the DFT calculations by examining the properties of bulk and slab models for MoS_2 as well as the structural properties of the thiophene molecule. Additionally, the performances of the set of Ni pseudopotentials provided in the VASP program to describe the bulk properties of Ni have been analyzed in great detail by Moroni et al.[30] Overall, based on the good agreement of the calculated properties of either bulk MoS_2 or the bare $MoS_2(0001)$ surface and of the Ni systems, it can be expected that the corresponding pseudopotentials are also accurate for the description of chemisorption properties of Ni−H_x and Ni−S_x complexes on the $MoS_2(0001)$ surface.

TABLE 1: Calculated Equilibrium Distances and the Adsorption Energies for Various Atomic Configurations Considered in the Present Study[a]

config.[b]	r(Mo−H)	r(S−H)	r(H−H)	E_{ads}
		(a) H_2 Adsorption		
free H_2			0.748	
1F		3.148	0.749	0.4
3F (h)		3.528	0.749	0.5
1F (def)	1.775	2.601	1.628	8.5
		(b) H Adsorption		
1F (v)		1.366		7.8
1F (t)	3.085	1.414		12.4
2H@1F		1.410	1.981	21.4
6F (out)	3.129	2.021		1.4
6F (in)	1.869	2.423		14.4
1F (def)	2.054	2.512		62.2

config.	θ	r(S−S*)	E_{ads}
	(c) S Adsorption		
1F	1/9	1.949	42.2
1F	2/9	1.942	41.0
1F	3/9	1.930	39.5
1F	5/9	1.917	38.8
1F	9/9	1.903	33.6

[a] Section a−c refer to adsorption of molecule H_2, atomic H and atomic S at different surface sites on the MoS_2(0001) surface. In the case of H and S studies results at different coverages θ are also indicated. All lengths and energies are shown in Å and kcal/mol, respectively. [b] The list of abbreviation used correspond to the following: 1F, 3F, and 6F indicate the 1-fold, 3-fold, and 6-fold surface sites; h, v, and t acronyms denote horizontal, vertical, or tilted adsorption configurations relative to surface plane; def. indicates adsorption at the sulfur 1F defective site; whereas 6F (out) and 6F (in) indicate two configurations of H at the 6F site, above the surface plane or in subsurface. S* denotes the adsorbed sulfur atom, whereas S denotes the surface sulfur atom.

III. Results and Discussions

A. Adsorption of H and S on MoS_2(0001). To examine the properties of Ni complexes including H and S on the basal plane of MoS_2, we first studied the adsorption properties of H_2, H, and S individually. In each case, the adsorption energy has been defined by

$$E_{ads} = \{NE_a + E_{slab} - E_{(a+slab)}\}/N \quad (1)$$

where E_a is the energy of the isolated adsorbate, E_{slab} is the total energy of the slab in the absence of the adsorbate, $E_{(a+slab)}$ is the total energy of the adsorbate/slab system, and N is the total number of adsorbate molecules in the supercell. A positive E_{ads} corresponds to a stable adsorbate/slab system. Unless otherwise noted, the results in this section are for a single adsorbate in a 3×3 surface unit cell, that is, a coverage of 1/9 ML.

Experimental studies[31,32] and previous theoretical results[19] have shown that under UHV conditions MoS_2 is unreactive toward molecular hydrogen. Our calculations are in agreement with this observation. We have examined a variety of binding sites for H_2 on the surface with various molecular orientations. Even the most favorable of these sites have binding energies less than 0.5 kcal/mol, corresponding to weak physisorption of the molecular species. The geometries and binding energies of H_2 adsorbed on surface 1-fold (1F) and 3-fold (3F) sites are summarized in Table 1.

For the adsorption of atomic H on MoS_2(0001), we found a number of locally stable adsorption sites. The main features of these sites are summarized in Table 1. When H is adsorbed on a surface S atom, H can bind either directly atop the S atom or in a tilted configuration in which the S−H bond makes an angle of 47.2° with the surface normal (see Figure 1, parts a and b). The tilted configuration is the more stable of these two sites, with a binding energy of 12.4 kcal/mol relative to the bare surface and a gas phase H atom. When H is located above the surface 6-fold (6F) site, there is a weakly bound state with H lying above the surface plane (not shown), and a considerably more stable state denoted 6F(in) in which H lies below the surface plane and is 3-fold coordinated to three Mo atoms (see Figure 1, parts c and f, for lateral and top views of this configuration). These two states are denoted 6F(out) and 6F(in), respectively, in Table 1. The 6F(in) state has a binding energy of 14.4 kcal/mol relative to gaseous H. The small binding energies of atomic H mean that dissociative adsorption of H_2 on the defect-free basal plane of MoS_2 is very unfavorable. For example, relative to the energy of the isolated slab and 1/2 $H_{2(g)}$, the 6F(in) site has a binding energy of −38.0 kcal/mol. Nonetheless, the existence of stable binding sites for H atoms suggests that if this species is created by some other process on the surface such as bond breaking at a step edge, then isolated H atoms may be found on the basal plane.

Additionally, we have studied the case when two H atoms are bonded to the same S surface atom (see Figure 1d and entry 2H@1F in Table 1). In this case, due to the attractive nature of H−H interaction, the binding energy increases to 21.4 kcal/mol per atom relative to the bare surface and the isolated gas-phase H atom. This configuration can be also seen as a H_2S molecule adsorbed at a vacancy site.

B. Formation and Influence of S Vacancies on MoS_2-(0001). There is a good deal of experimental and theoretical evidence that S vacancies on the basal plane of MoS_2 create more stable binding sites for adsorbed species than exist on the basal plane itself.[17,20,31] Additionally, it has been shown[31,32] that such vacancies can be easily formed upon exposure of the MoS_2 surface to gas-phase hydrogen atoms, following the reaction $2H(gas) + S(surf) \rightarrow H_2S(gas)$. This reaction was found to be very effective for removal of sulfur atoms from the MoS_2(0001) surface leading to formation of anion vacancies.[32] To complement these studies, we have performed a number of calculations to understand the formation of S vacancies on MoS_2(0001) and to determine the interaction of atomic and molecular hydrogen with such vacancies.

We first considered the process of S vacancy formation by calculating the potential energy path for desorption of H_2S from a surface partly covered with adsorbed H atoms. The corresponding potential profile is depicted in Figure 2. The initial state considered corresponds to two H atoms adsorbed at the same S site, whereas a desorbed H_2S molecule represents the final state. These calculations yield an activation energy for H_2S extraction of about 18 kcal/mol. This value is very close to the activation energy of 17.5 kcal/mol suggested by Diez and Jubert[33] based on extended Hückel molecular orbital calculations. This process has been also examined experimentally by Wiegenstein and Schulz in experiments where the surface is exposed to atomic deuterium.[31] Their TPD experiments indicate that the activation energy of D_2S desorption is 39.4 kcal/mol, a value much larger than the one suggested by our calculations. The source of this discrepancy is unclear. Our calculations indicate that the net energy change in creating a S vacancy by formation of H_2S is less than 2 kcal/mol. This occurs because the formation energy of H_2S almost compensates for that of creating a S vacancy on the surface.

We analyzed the adsorption of a H_2 molecule at a S vacancy on the MoS_2(0001) surface using the same supercell as in our

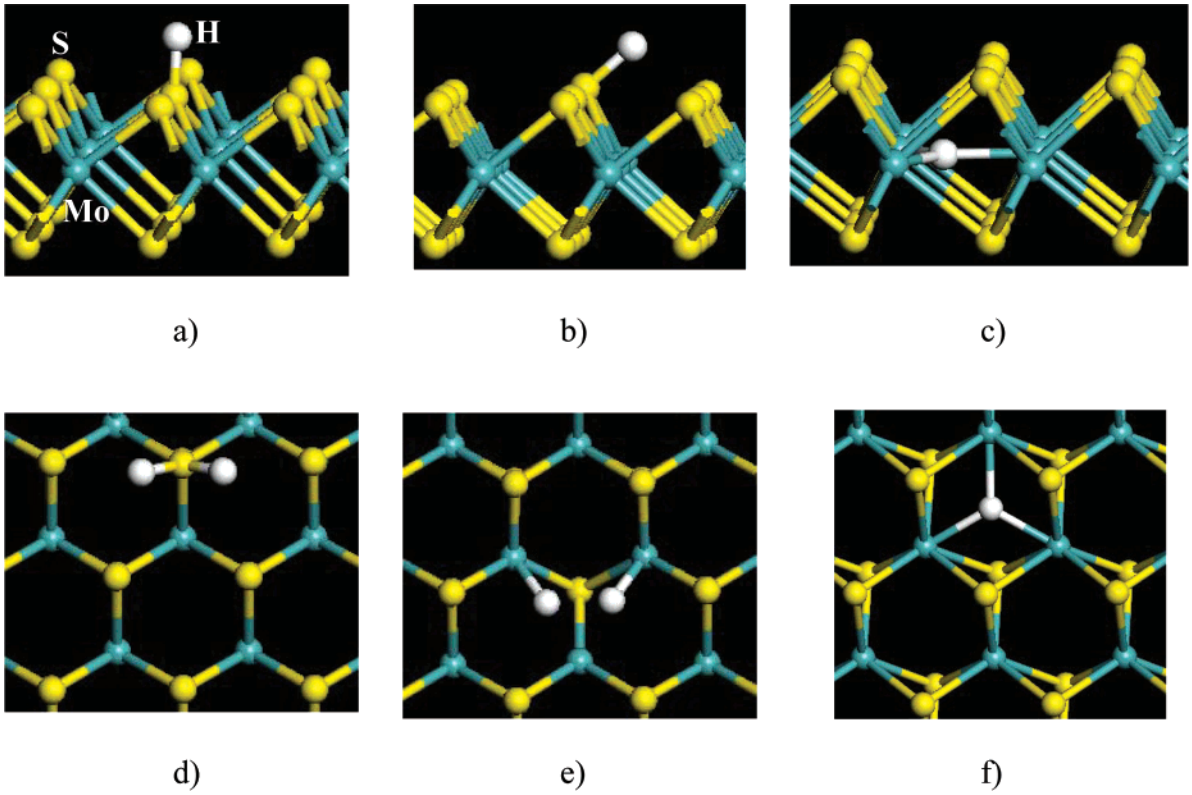

Figure 1. Pictorial representation of the lateral and top views of the main adsorption configurations of H and H_2 on MoS_2(0001) surface: (a) on top of sulfur atoms, (b) in a tilted configuration with H oriented toward the 6-fold hollow site, (c) subsurface 6F configuration (lateral view configuration), (d) two H atoms adsorbed on the same sulfur atom, (e) dissociative adsorption of H_2 at a sulfur vacancy, (f) subsurface 6F configuration (top view configuration). For visualization purposes this latest configuration is slightly rotated from surface normal direction.

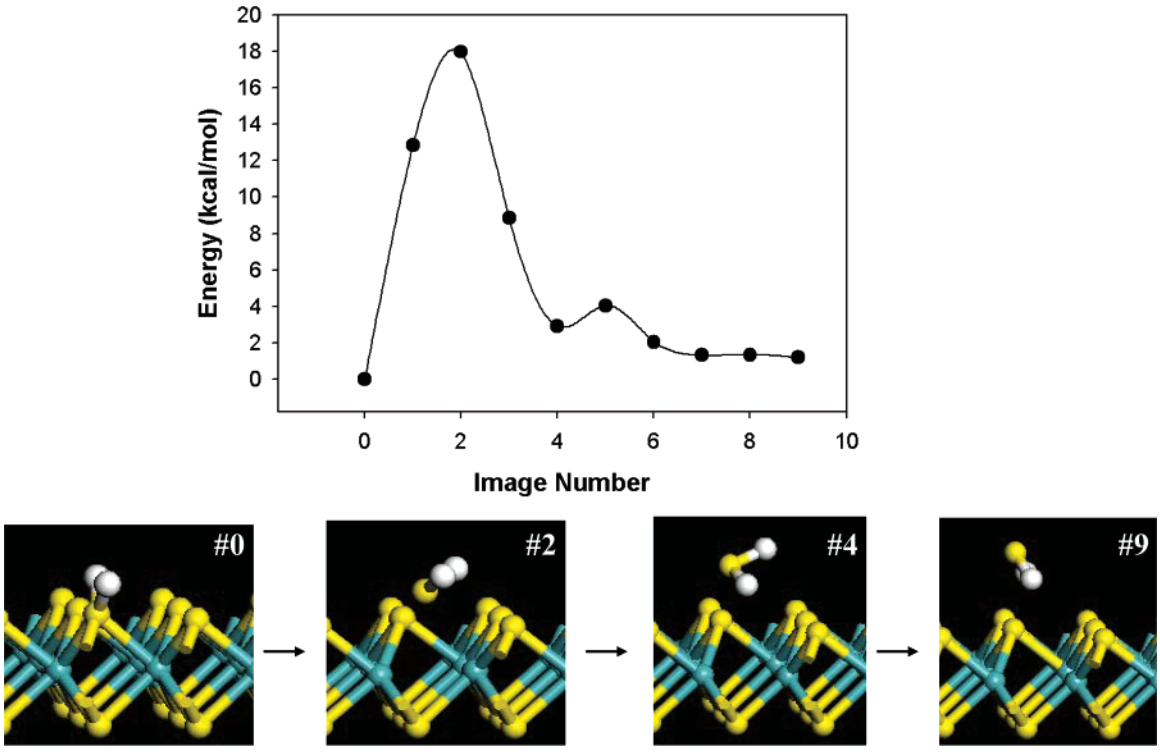

Figure 2. Potential energy surfaces for extraction of H_2S from MoS_2 (0001) surface with desorption of H_2S(g) and formation of a S vacancy.

previous calculations of Ni adsorption in S vacancies.[20] The S vacancy was made by simply removing one S atom from the top S layer in the slab model. Geometry optimization of an H_2 molecule placed near this defect site shows the existence of an adsorption state in which the molecule dissociatively chemisorbs on the surface (see Figure 1e). In this configuration, H atoms bind to two neighbor Mo atoms at about 1.792 Å from these atoms. The lateral separation between the H atoms is 1.628 Å. The corresponding adsorption energy per H atom is 8.5 kcal/mol relative to the energies of the isolated surface and H_2 molecule or 56.7 kcal/mol relative to the energies of isolated surface and two H atoms.

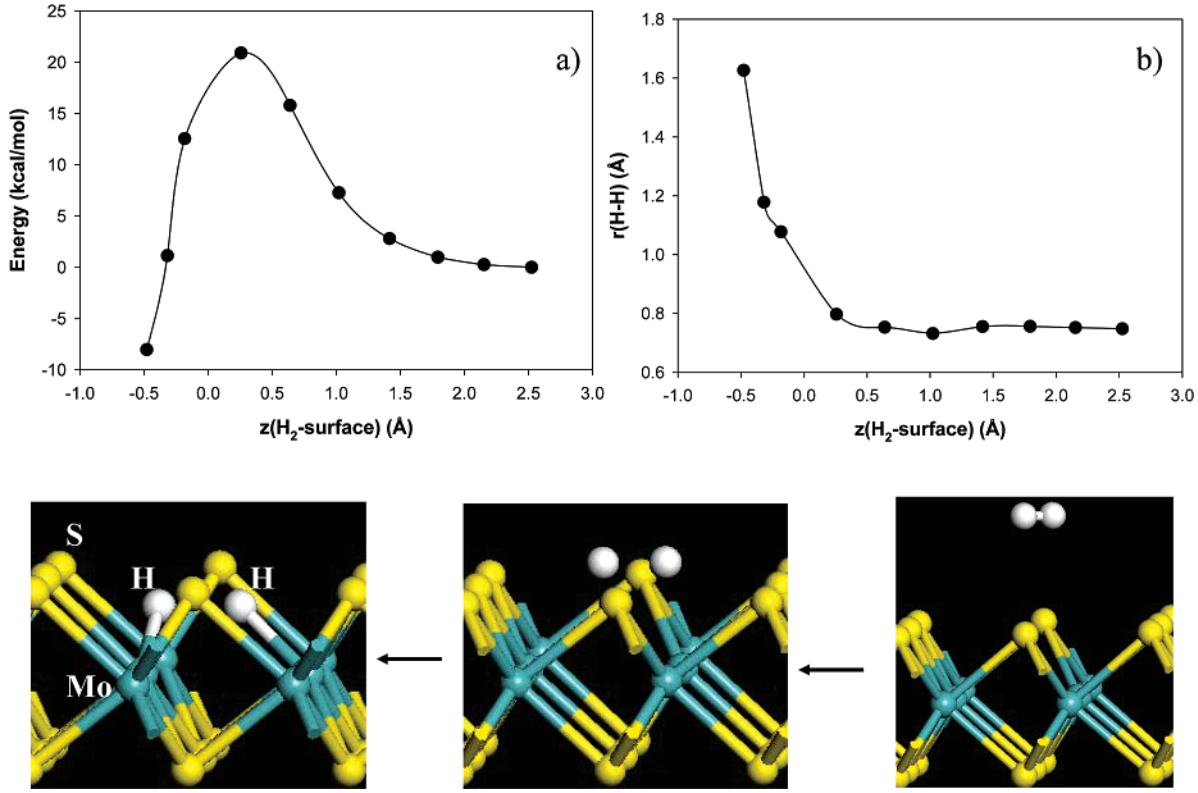

Figure 3. (a) Potential energy surface for dissociation of H_2 molecule at a defective S site. (b) Variation of the H−H bond along the reaction path as function of the vertical distance to the MoS_2 surface.

To determine the minimum energy path for dissociative adsorption of H_2 at a S vacancy, we used the NEB method with the initial state corresponding to a H_2 molecule oriented parallel to the surface at about 2.5 Å from the surface and the dissociatively chemisorbed state at the defective site as the final state. The minimum energy path corresponding to this process is represented in Figure 3a. This calculation indicates that a barrier of about 22 kcal/mol must be overcome in order to dissociatively chemisorb H_2 at a S vacancy. During this dissociation process, the corresponding H−H bond length elongates from the equilibrium value of 0.74 to 1.62 Å in the final adsorbed state (see Figure 3b).

Finally, in the case of a surface with S vacancies, an H atom can also adsorb at the defective site. The adsorption configuration (denoted with 1F(def) in Table 1) corresponds to a subsurface, symmetric position of H atom relative to the three neighbor Mo atoms with a Mo−H separation of 2.054 Å and above a S atom from the bottom layer at a distance of 2.512 Å. As should be expected from the discussion above of H_2 dissociation at S defects, the binding energy for atomic H in this configuration, 62.2 kcal mol relative to gas-phase H, is much larger than the binding energies of atomic H on the defect free basal plane.

C. Diffusion Properties of Atomic H on MoS_2(0001). To understand the mobility of atomic H on the basal plane relative to the Ni complexes considered below, we have performed a number of NEB calculations to determine the activation energies associated with diffusion of an isolated H atom on the surface. The minimum energy paths (MEPs) for H diffusion along different pathways are presented in Figure 4. Figure 4a corresponds to the diffusion of H among two 1F vertical adsorption configurations. Along this pathway the atom passes through two 1F tilted configurations. As can be seen from this figure, the vertical and tilted 1F configurations are separated by a small barrier of about 1.5 kcal/mol, whereas the barrier between tilted 1F configurations is about 7 kcal/mol. Similar diffusion barriers of 6−7 kcal/mol are seen in the case when diffusion is started from a tilted 1F(t) configuration and ends up in a 1F(t) configuration in the next surface unit (see Figure 4b). This pathway involves only passage through 1F(t) type of local minima. The intermediate and final minima in Figure 4b correspond to the H atom being bonded on opposite sites of a surface S atom.

A final diffusion pathway for atomic H (not shown) we have considered is the diffusion of H atom from the tilted 1F configuration toward the bulk to the 6F(in) adsorption configuration. In this case, we find that the transition state for diffusion lies above the energy required to simply desorb atomic H from the 1F binding site. Further examining the MEP for adsorption of atomic H into the 6F(in) configuration from the gas phase showed that H must surmount a barrier 3.4 kcal/mol above the energy of the desorbed state in order to enter the 6F(in) site. These results indicate that, at low temperatures such as those used in the experiments of Weiss et al.,[16−18] if atomic H is present on the basal plane then it is likely to exist primarily in the 1F binding sites. Moreover, diffusion of atomic H among these sites is relatively facile, because it can occur via a series of mechanisms with activation energies of 7 kcal/mol and less. For practical applications such as hydrodesulfurization, this aspect is important as the basal plane can act as a hydrogen reservoir that replenished the corresponding edge sites where reactions take place.

Beside H atoms, we have also characterized the interaction of isolated S atoms with the MoS_2 basal plane. In this case we found (see Table 1, section c) that atomic sulfur can adsorb on top of surface S atoms at a distance of about 1.949 Å in the low coverage limit. The corresponding adsorption energy is 42.2 kcal/mol. Other initial configurations at 3F or 6F sites evolve to the 1F configuration, on top of surface S atoms. For the adsorption at the 1F site, we have also performed calculations

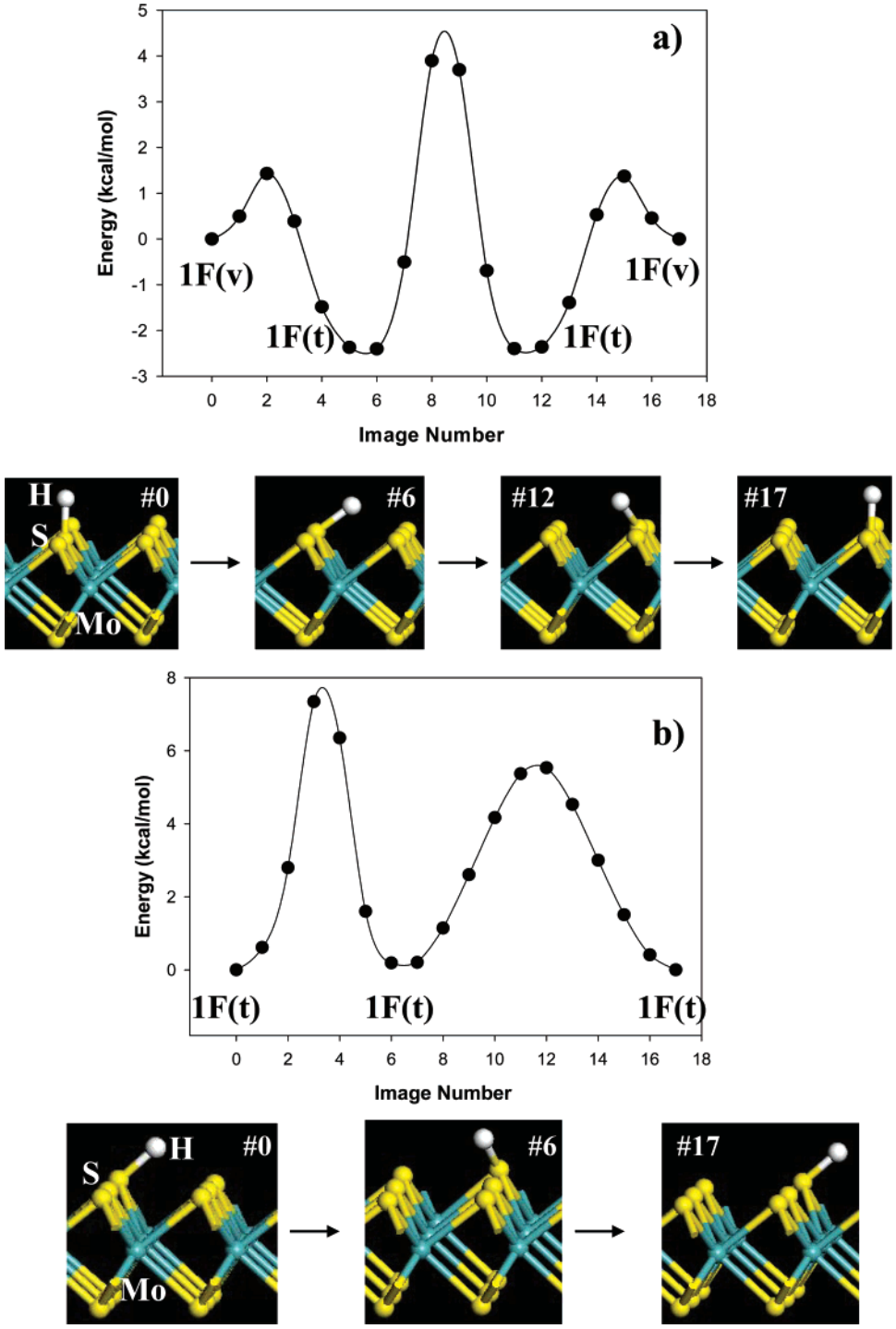

Figure 4. Potential energy surface for diffusion of H atoms along the pathways: (a) 1F (v) → 1F(t) → 1F(t) → 1F(v); (b) 1F(t) → 1F(t) → 1F(t). 1F(v) and 1F(t) correspond to vertical and tilted configurations of H atom on top of S atom at a 1F site, respectively.

as a function of coverage (see data in Table 1). The S coverage was varied from 1/9 to 1 by placing S atoms in the 3×3 surface unit cell such as to minimize the lateral interactions between the neighboring S adatoms at each coverage. The binding energy of S decreases almost linearly with coverage up to the full coverage. The corresponding dependence of coverage Θ was found to be of the form $E(\Theta) = 43.2 - 9.3\Theta$ with the energy expressed in kcal/mol.

D. Formation of NiX Complexes on MoS_2(0001). In our previous study related to adsorption and diffusion properties of Ni atoms on MoS_2(0001) surface,[20] we analyzed three major adsorption configurations for the Ni atoms on the basal plane. The first one, denoted 1F (see Figure 3 in ref 20), corresponds to Ni atom adsorbed on top of the sulfur atoms. The second one, denoted 6F, is a 6-fold hollow site in which the Ni atom is surrounded by three Mo and three S atoms. The last one, denoted 3F, corresponds to adsorption on top of a Mo atom with a 3-fold binding to neighbor sulfur atoms. For consistency in the current paper we will continue to denote these sites as 1F, 6F and 3F, respectively. Our calculations indicate a stability order of $E_{ads}(3F) > E_{ads}(6F) > E_{ads}(1F)$ with a binding energy of about 77 kcal/mol for the most stable adsorption configuration at 3F site.

We have calculated the energy of NiX complexes (X = H, H_2, S, S_2, SH, and H_2S) adsorbed in each of the three Ni binding sites defined above. Pictorial views of these complexes are given

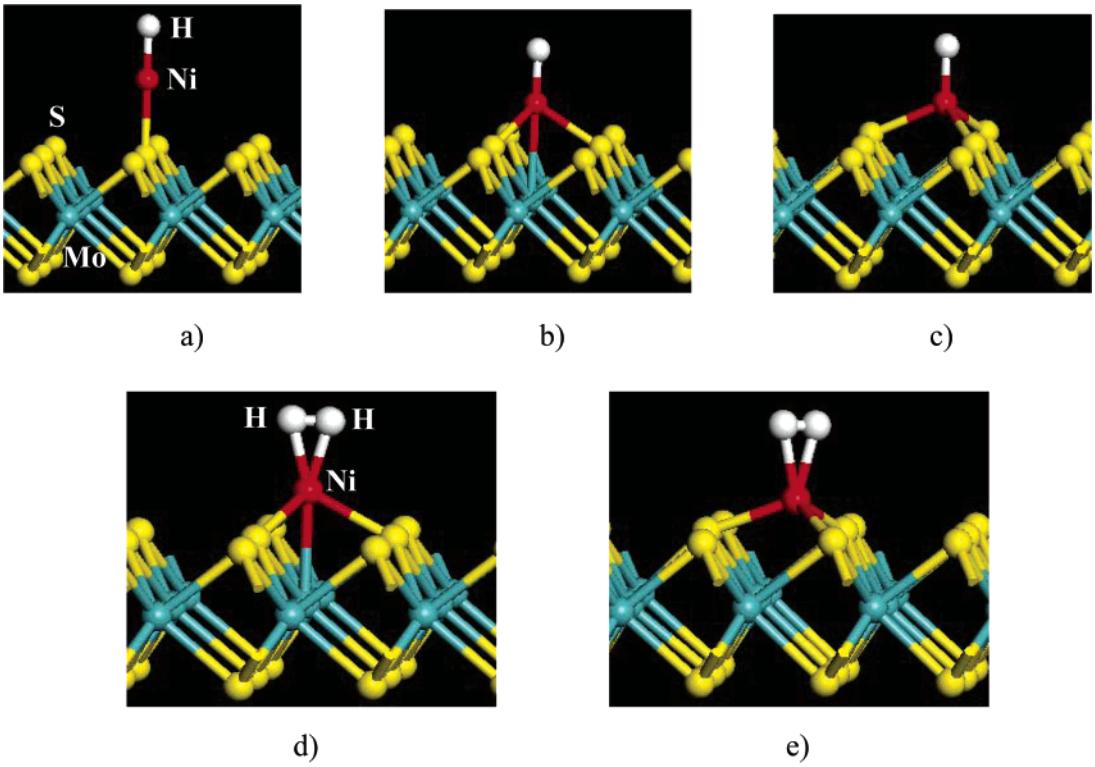

Figure 5. Pictorial representation of the adsorption configuration of atomic hydrogen on Ni atom positioned at: (a) on-top (1F) of sulfur atom, (b) 3-fold (3F) site, (c) 6-fold (6F) configuration. Panels d and e represent molecular hydrogen adsorbed at Ni(3F) and Ni(6F) sites.

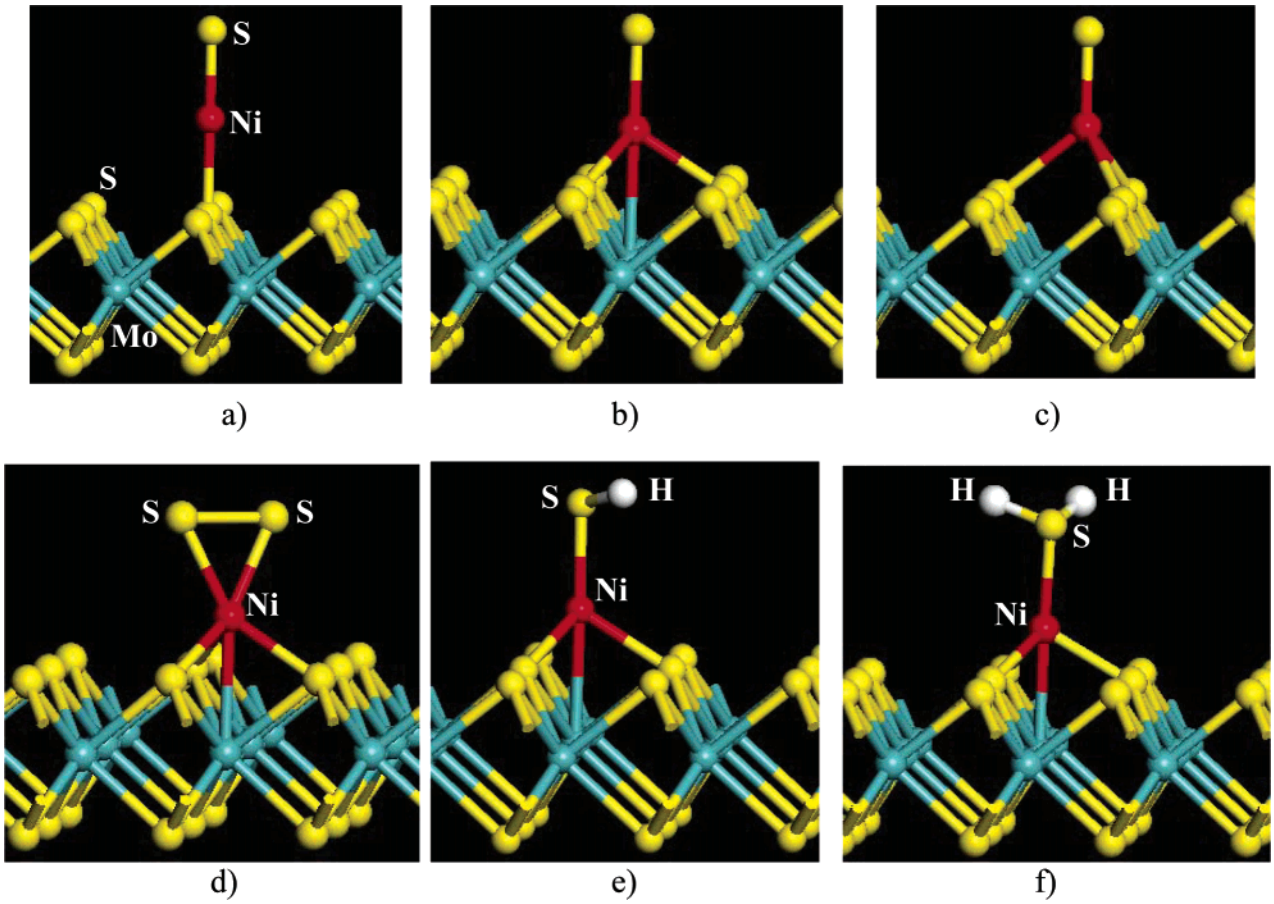

Figure 6. Pictorial representation of the adsorption configurations of S on top of Ni atom at (a) 1F site, (b) 3F site, (c) 6F site. Panels d−f present configurations of S_2, SH, and H_2S adsorbed on Ni atom at 3F site.

in Figures 5 and 6. For each complex, there are two binding energies of interest, the binding energy of X to the Ni atom, denoted E_{1ads} below, and the binding energy of the entire complex to the surface, denoted E_{2ads}. These two binding

TABLE 2: Calculated Equilibrium Distances and the Adsorption Energies for Various Atomic Configurations of H, H_2, S, S_2, and H_2S Adsorbed on Ni/MoS_2(0001)[a]

config.	r(Mo−Ni)	r(S−Ni)	r(Ni−X)[b]	r(X−X)	E_{1ads}[c]	E_{2ads}[c]
			USPP Results			
			Ni Adsorption[d]			
1F	4.006	1.969				33.9
3F	2.590	2.123				77.6
6F	2.864	2.066				67.0
			(a) Ni−H Adsorption			
free Ni−H			1.471			
1F	4.152	2.156	1.520		59.5	23.4
3F	2.689	2.176	1.509		40.5	48.0
6F	3.093	2.142	1.510		38.7	35.7
			(b) Ni−H_2 Adsorption			
free Ni-2H			1.427			
3F	2.623	2.169	1.676	0.820	14.4	73.5
6F	2.993	2.141	1.721	0.807	9.2	57.9
			(c) Ni−S Adsorption			
free Ni−S			1.977			
1F	4.171	2.185	2.007		86.4	23.9
3F	2.742	2.229	2.053		63.0	44.2
6F	3.590	2.355	2.036		58.3	29.1
			(d) Ni−S_2 Adsorption			
free Ni−S_2			2.106	2.084		
1F	3.959	2.117	2.159	2.033	67.6	31.4
3F	2.778	2.235	2.252	1.995	31.9	39.4
			(e) Ni−SH Adsorption			
free Ni−SH			2.064			
3F	2.707	2.212	2.145		50.9	49.8
6F	3.560	2.325	2.134		45.5	34.1
			(f) Ni−H_2S Adsorption			
free Ni−H_2S			1.984			
3F	2.640	2.175	2.238		23.0	72.5
6F	3.113	2.147	2.281		15.4	43.6
			PAW Results			
			Ni Adsorption[d]			
1F	3.991	1.958				40.6
3F	2.581	2.121				80.6
6F	2.819	2.068				71.8
			(g) Ni−H Adsorption			
free Ni−H						
1F	4.141	2.144	1.507		55.3	26.6
3F	2.690	2.172	1.500		40.9	52.2
6F	2.996	2.129	1.497		39.1	41.5
			(h) Ni−H_2 Adsorption			
free Ni-2H			1.427			
3F	2.619	2.168	1.654	0.829	15.0	68.6
			(i) Ni−S Adsorption			
free Ni−S			1.955			
3F	2.732	2.238	2.037		64.9	40.9
			(j) Ni−S_2 adsorption			
free Ni−S_2			2.095	2.076		
3F	2.743	2.222	2.232	2.000	33.4	39.7

[a] All lengths and energies are shown in Å and kcal/mol, respectively. [b] Abbreviation X stands for H or S symbols. [c] The energy E_{1ads} corresponds to adsorption energy of adsorbate X (X = H or S) on Ni/MoS_2(0001), whereas energy E_{2ads} represents the adsorption energy of Ni−X complex on MoS_2(0001) surface. [d] These values refer to adsorption of single Ni atoms on MoS_2(0001) and have been taken from ref 20.

energies are summarized, along with several bond lengths, for each complex in Table 2. It can be seen from this table that H, S, S_2, and SH all bind strongly to Ni on the MoS_2 basal plane, with values of E_{1ads} exceeding 40 kcal/mol for Ni in its 3F site. The binding energy of H on Ni(3F) is similar to those reported for adsorption of H on metal sites of nickel sulfide clusters (43−61 kcal/mol).[34] H_2 and H_2S also bind to Ni in the 3F site, although less strongly, with E_{1ads} = 14.4 and 23.0 kcal/mol, respectively. It is noteworthy that this binding energy for H_2 is quite large compared with the binding energy of H_2 on the unmodified surface, so the presence of Ni adatoms on the basal plane will substantially increase the lifetime of H_2 on the surface in environments where gas-phase H_2 is present. The calculated value corresponding to H_2 adsorption on Ni at a 3F site is close to the one reported previously by Rodriguez,[19] based on unrestricted Hartree−Fock calculations, of 13.8 kcal/mol. For every complex, the 3F site is found to be the energetically preferred location for the adsorbed complex. In several cases, either the 1F or 6F is not a local minimum for the adsorbed complex and systems initialized in these geometries spontaneously moved to one of the other stable minima during geometry optimization.

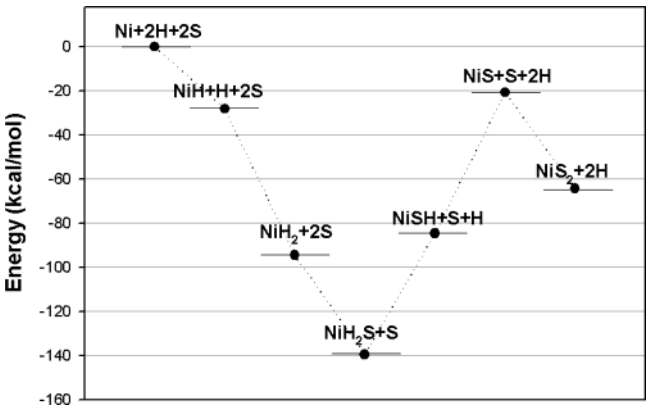

Figure 7. Diagram of the relative energies of various Ni−X complexes (X = H, H_2, S, S_2, SH, and H_2S) considered in text. The energy reference corresponds to the case of adsorbed, well-separated atoms.

When the binding energy of the complexing atoms to the surface Ni atom is strong, there is a tendency for the adsorption energy of the entire complex to the surface to be weakened. Examining the values of E_{2ads} listed in Table 2 shows that for H, S, S_2, and SH, E_{2ads} is 20−30 kcal/mol less than for a bare Ni in a 3F site. For H_2 and H_2S, these energy differences are much less. As we will show below, these changes in the binding energy of the cluster with the surface have strong implications for the diffusion of these complexes on the surface.

To compare the relative energies of the various complexes, we can examine $E_{NiH_xS_y(a)} + (2 - x)E_{H(a)} + (2 - y)E_{S(a)} + (4 - x - y)E_{bare}$, where $E_{C(a)}$ and E_{bare} are the total energy of a supercell with the species C adsorbed on the MoS_2 surface and the total energy of a supercell containing only the MoS_2 surface, respectively. The relative energies calculated as

$$\{E_{NiH_xS_y(a)} + (2 - x)E_{H(a)} + (2 - y)E_{S(a)} + (4 - x - y)E_{bare}\} - \{E_{Ni(a)} + 2E_{H(a)} + E_{S(a)}\}$$

are shown in Figure 7. Here the energy of the system with all of the adsorbed atoms well separated on the surface, namely $E_{Ni(a)} + 2E_{H(a)} + 2E_{S(a)}$, has been taken as reference. The results given in Figure 7 indicate that the most energetically stable complex among the set we have considered is NiH_2S. Figure 7 also shows, for example, that if Ni and H atoms are present on a basal plane under conditions that are not kinetically limited the surface population of NiH_2 will greatly exceed that of NiH or isolated Ni adatoms. To fully understand the conversion rates between the various complexes possible on surfaces with Ni, H, and S adsorbates, it is of course necessary to determine the energy barriers between the states shown in Figure 7. We have

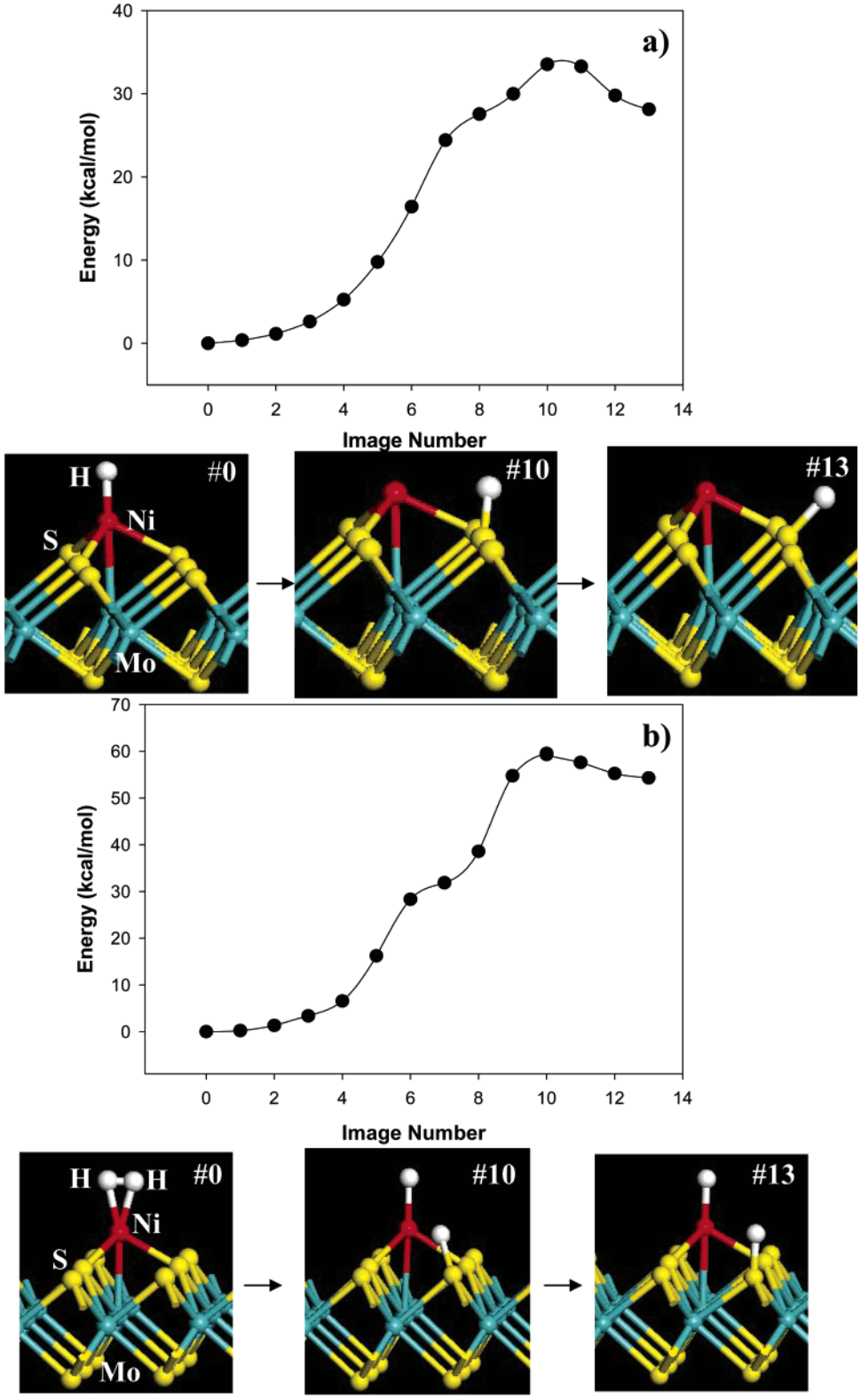

Figure 8. (a) Potential energy surface for Ni(3F)-H dissociation with formation of S−H bond. (b) Potential energy surface for dissociation of H_2 molecule adsorbed on Ni(3F) atom with formation of Ni(3F)−H and S−H products. The indicated atomic configurations correspond to reactant, transition state and product configurations.

determined these barriers for the two complexes that involve only Ni and H. The MEP for conversion between a NiH complex adsorbed in a 3F site and Ni in the same 3F site with H bonded to an adjacent surface S atom in the 1F(t) configuration is shown in Figure 8a. The energy barrier to form the complex is around 7 kcal/mol, very similar to the activation energy for diffusion of isolated H atoms on the surface. The barrier for the reverse process is much larger because of the strong relative stability of the adsorbed complex. A similar situation exists for the conversion between an adsorbed NiH_2 complex and a NiH complex with an adjacent adsorbed H atom. The MEP for this process is shown in Figure 8b. In this case, the barrier to form the NiH_2 complex is around 5 kcal/mol. We have also analyzed the case when H_2 adsorbs on the Ni atom coming directly from

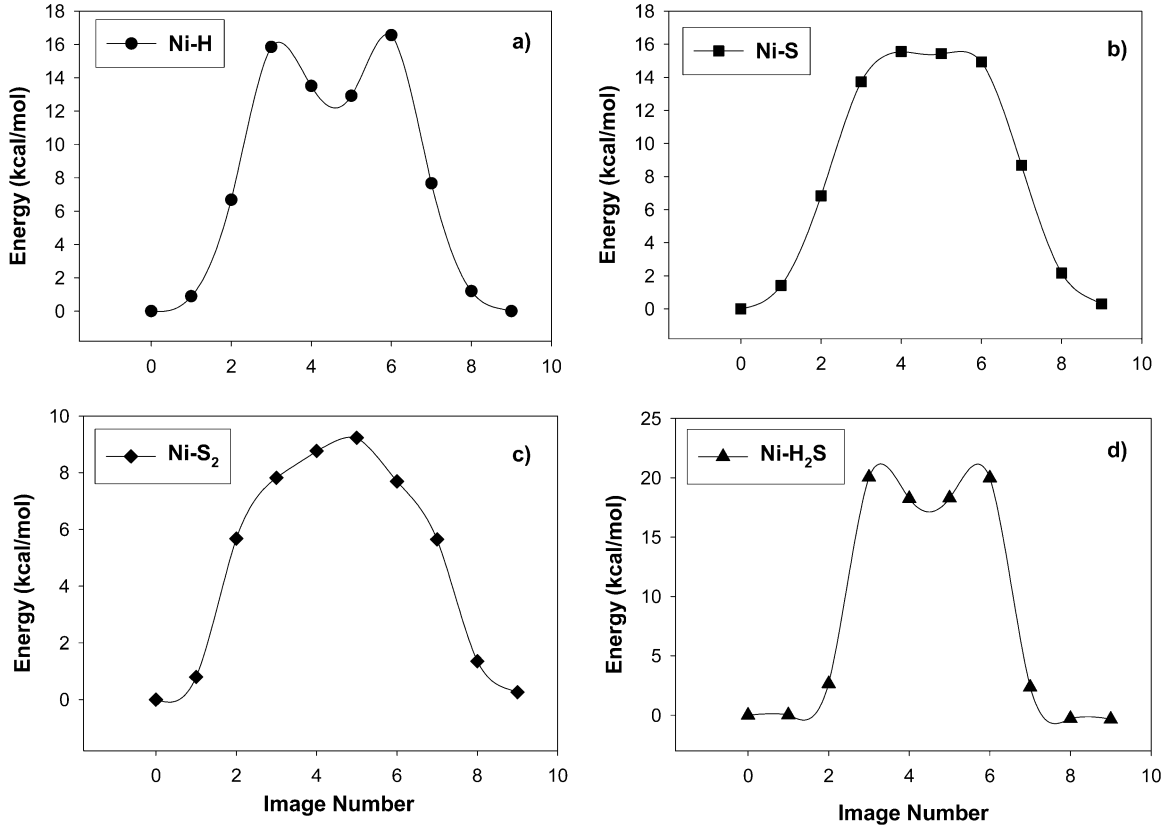

Figure 9. Potential energy surface for diffusion of (a) Ni−H, (b) Ni−S, (c) Ni−S_2, and (d) Ni−H_2S complexes between 3F adsorption sites.

the gas phase. In this case, our results (not shown) indicate that there is no activation barrier for chemisorption. These results indicate that a major role of Ni atoms on the MoS_2 basal plane is to increase the amount of hydrogen adsorbed on the surface either in the molecular or atomic forms. Additionally, the Ni atoms can serve as centers for dissociation of molecular H_2 leading to adsorbed H species with formation of Ni−H and S−H bonds.

In Table 2, we also analyze the modifications of some of the results above for the case when the projector augmented method (PAW)[27,28] is used instead of the ultrasoft pseudopotentials. As can be seen from sections g and h of Table 2, the calculated binding energies of either H or H_2 on the Ni atom are slightly larger than those obtained using USPs (see sections a and b in Table 2). However, the corresponding geometrical parameters obtained based on the two methods are very similar. We can conclude that the two methods provide similar data on the energetic and geometric parameters of atomic and molecular hydrogen adsorbed on Ni atoms at different surface sites.

E. Diffusion of NiX Complexes on MoS_2(0001). In our previous study,[20] we have analyzed three different diffusion pathways of isolated Ni atoms on the MoS_2 basal plane suggested by the surface symmetry: 3F → 1F, 3F → 6F → 3F, and 3F → 6F → 1F. Among these pathways, we found that diffusion along the 3F → 6F → 3F pathway has the smallest barrier with a value of 20.1 kcal/mol. In the present study, we extended these investigations by considering diffusion of the NiH_xS_y complexes described above. Because we showed above that all of these clusters adsorb most favorably in 3F surface sites, we have examined diffusion between adjacent 3F sites. In each case, we calculated minimum energy paths using the NEB method[29] with 8 images distributed between the end points.

The calculated minimum energy paths for NiH, NiS, NiS_2, and NiH_2S are shown in Figure 9. The activation energies for the diffusion of all of the complexes we have considered relative to the stable 3F site, together with the result for a bare Ni atom, are summarized in Figure 10. The presence of complexing atoms on the adsorbed Ni typically reduces the activation energy for diffusion. In Figure 10, this observation is shown by plotting the diffusion activation energies as a function of the binding energy of the relevant complex on the surface, E_{2ads}. The most dramatic example is the diffusion activation energy of NiS_2, which is roughly 10 kcal/mol less than the activation energy for diffusion of an isolated Ni atom.

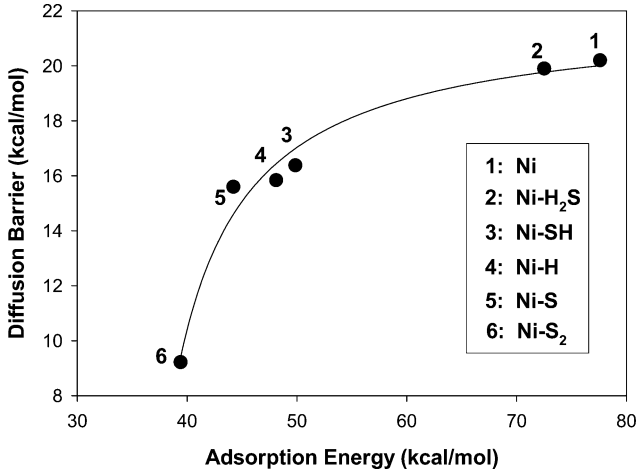

Figure 10. Variation of the calculated diffusion barriers for Ni atom and Ni-X complexes (X = H_2S, SH, H, H_2, S, and S_2) as function of the corresponding binding energy at 3F sites.

We can now discuss whether any of the complexes discussed above can be identified as the rapidly diffusing surface species observed in the STM experiments of Weiss et al. at 77 K.[16−18] The DFT-predicted diffusion activation energies for NiX complexes described above are all larger than the DFT-predicted

activation energy for diffusion of atomic H on the MoS_2 basal plane. If we consider atomic H as a prototypical fast diffusing species, then its activation energy of 7 kcal/mol yields a hopping time on the surface of 10^{-8} s at 300 K, assuming a hopping attempt frequency of 10^{13} s^{-1}. This hopping time increases enormously at the cryogenic temperatures used by Weiss et al.; at 77 K the equivalent hopping time exceeds 10^6 s. Even if the hopping attempt frequency is several orders of magnitude larger than 10^{13} s^{-1}, our results indicate that H diffuses extremely slowly on the MoS_2 basal plane at 77 K. Because the direct hopping diffusion mechanisms of all of the NiX complexes we examined have larger activation energies than atomic H, we must conclude that none of these mechanisms can be identified with the rapid diffusion observed by Weiss et al.[16−18] using STM at 77 K.

IV. Conclusions

We have used plane wave DFT to examine the adsorption and diffusion properties of H, H_2, and S species and of $Ni-H_x$ and $Ni-S_x$ ($x = 1,2$) complexes on $MoS_2(0001)$. Our main results can be summarized as follows:

(a) On nondefective surfaces, H_2 adsorption is extremely weak. However, adsorption is possible in the case of a surface with S defective sites. In this case, adsorption can take place dissociatively with formation of Mo−H bonds.

(b) Atomic hydrogen can adsorb on the nondefective surface with formation of either S−H or Mo−H bonds. In the first case, we have identified two adsorption configurations: a vertical ($E_{ads} = 7.8$ kcal/mol) and a tilted ($E_{ads} = 12.4$ kcal/mol) configuration. In the latter case, the S−H bond is oriented toward the 6F hollow site. An even more stable configuration ($E_{ads} = 21.4$ kcal/mol per atom) was identified when two H atoms adsorb at the same S site. The indicated energies are calculated with respect to the bare surface and the isolated H atom. Finally, we determined adsorption configurations where Mo−H bonds can be formed. This is the case of a subsurface configuration beneath the 6F site (with a binding energy of 14.4 kcal/mol) in which H atom symmetrically bonds with three Mo atoms. Another configuration was seen for the case of a defective surface where Mo−H bonding takes place with an adsorption energy of 62.2 kcal/mol. We have also analyzed the possibility of S extraction from the surface with formation of $H_2S(g)$ and a S vacancy and shown that such a process requires about 18 kcal/mol.

(c) S atoms can bind on top of surface S atoms, but the adsorption energy is coverage dependent. We have determined a linear dependence for the binding energy of coverage Θ ($1/9 < \Theta < 1$) of the form $E(\Theta) = 43.2-9.3\Theta$, with energy expressed in kcal/mol.

(d) Ni atoms present on the surface represent centers of enhanced chemical activity where H, H_2, S, S_2, HS, and H_2S species can be adsorbed with significant bonding energies. As a result of decoration of Ni atoms with these chemical species, the interaction of the Ni atoms with the surface decreases. For example, for the Ni atoms adsorbed at the 3F site, the binding energy decreases from 77 kcal/mol to 48.1 kcal/mol as a result of H adsorption or to 39.4 kcal/mol as a result of S_2 adsorption.

(e) By assuming a direct hopping mechanism for NiX (X = H, H_2, S, S_2, HS, and H_2S) complexes, we have evaluated the diffusion barriers for these complexes between 3F adsorption sites. Our results indicate that these complexes have smaller diffusion barriers than the bare Ni atoms. The smallest barriers have been seen for NiS_2 (9.2 kcal/mol), NiS (15.6 kcal/mol), and NiH (15.9 kcal/mol) systems. These barriers are all smaller than those obtained in the case of bare Ni atom diffusion of 20 kcal/mol. These diffusion barriers suggest that these complexes will diffuse rapidly at room temperature but extremely slowly at cryogenic temperatures. These findings indicate that by adsorption of H or S species the mobility of Ni atoms on the $MoS_2(0001)$ basal plane increases.

Acknowledgment. We gratefully acknowledge the supercomputer allocation provided by Pittsburgh Supercomputer Center under the $(SC)^2$ partnership program. D.S.S. is an ORISE Faculty Fellow at NETL and an Alfred P. Sloan fellow.

References and Notes

(1) Topsøe, H.; Clausen, B. S.; Franklin, F. E.; Massoth, E. In *Science and Technology in Catalysis: Hydrotreating Catalysis*; Anderson, J. R., Boudart, M., Eds.; Springer: Berlin, 1996; Vol. 11.
(2) Kabe, T.; Ishihara, A.; Qian, W. *Hydrodesulfurization and Hydrodenitrogenation: Chemistry and Engineering*; Wiley: New York, 2000.
(3) Prins, R.; De Beer, V. H. J.; Somorjai, G. A. *Catal. Rev. Sci. Eng*. **1989**, *31*, 1.
(4) Tauster, S. J.; Pecoraco, T. A., Chianelli, R. R. *J. Catal*. **1980**, *63*, 515.
(5) Byskov, L. S.; Nørskov, J. K.; Clausen, B. S.; Topsøe, H. *J. Catal*. **1999**, *187*, 109.
(6) Helveg, S.; Lauritsen, J. V.; Lægsgaard, S.; Stensgaard, I.; Nørskov, J. K.; Clausen, B. S.; Topsøe, H.; Besenbacher, F. *Phys. Rev. Lett*. **2000**, *84*, 951.
(7) Lauritsen, J. V.; Helve, Lægsgaard, S.; Stensgaard, I., Clausen, B. S.; Topsøe, H.; Besenbacher, F. *J. Catal*. **2001**, *197*, 1.
(8) Lauritsen, J. V.; Nyberg, M.; Vang, R. T.; Bollinger, M. V.; Clausen, B. S.; Topsøe, H.; Jacobsen, K. W.; Lægsgaard, E.; Nørskov, J. K.; Besenbacher, F. *Nanotechnology* **2003**, *14*, 385.
(9) Raybaud, P.; Hafner, J.; Kresse, G.; Toulhoat, H. *Surf. Sci*. **1998**, *407*, 237.
(10) Raybaud, P.; Hafner, J.; Kresse, G.; Toulhoat, H. *Phys. Rev. Lett.* **1998**, *80*, 1481.
(11) Raybaud, P.; Hafner, J.; Kresse, G.; Kasztelan, S.; Toulhoat, H. *J. Catal.* **2000**, *189*, 129.
(12) Raybaud, P.; Hafner, J.; Kresse, G.; Kasztelan, S.; Toulhoat, H. *J. Catal.* **2000**, *190*, 128.
(13) Schweiger, H.; Raybaud, P.; Kresse, G. Toulhoat, H. *J. Catal*. **2002**, *207*, 76.
(14) Schweiger, H.; Raybaud, P. Toulhoat, H. *J. Catal*. **2002**, *212*, 33.
(15) Salmeron, M.; Somorjai, G. A.; Wold, A. Chianelli, R.; Liang K. S. *Chem. Phys. Lett*. **1982**, *90*, 105.
(16) Kushmerick, J. G.; Weiss, P. S. *J. Phys. Chem. B* **1998**, *102*, 10094.
(17) Kushmerick, J. G.; Han, K. P.; Johnson, J. A.; Weiss, P. S. *J. Phys. Chem. B* **2000**, *104*, 2980.
(18) Kandell, S. A.; Weiss, P. S. *J. Phys. Chem. B* **2001**, *105*, 8102.
(19) Rodriguez, J. A. *J. Phys. Chem B* **1997**, *101*, 7524.
(20) Sorescu, D. C.; Sholl, D. S.; Cugini, A. V. *J. Phys. Chem. B* **2003**, *107*, 1988.
(21) Kresse, G.; Hafner, J. *Phys. Rev*. **1993**, *B 48*, 13115.
(22) Kresse, G.; Furthmüller, J. *Comput. Mater. Sci*. **1996**, *6*, 15.
(23) Kresse, G.; Furthmüller, J. *Phys. Rev.* **1996**, *B 54*, 11169.
(24) Vanderbilt, D. *Phys. Rev.* **1990**, *B 41*, 7892.
(25) Kresse, G.; Hafner, J. *J. Phys. Condens. Matter* **1994**, *6*, 8245.
(26) Perdew, J. P.; Chevary, J. A.; Vosko, S. H.; Jackson, K. A.; Pedersen, M. R.; Singh, D. J.; Frolhais, C. *Phys. Rev.* **1992**, *B 46*, 6671.
(27) Blöch, P. E. *Phys. Rev*. **1994**, *B50*, 17953.
(28) Kresse, G.; Joubert, D. *Phys. Rev*. **1999**, *B59*, 1758.
(29) Mills, G.; Jónsson, H.; Schenter, G. K. *Surf. Sci.* **1995**, *324*, 305.
(30) Moroni, E.; Kresse, G.; Hafner, J.; Furtmüller, J. *Phys. Rev.* **1997**, *B 56*, 15629.
(31) Wiegenstein, C. G.; Schulz, K. H. *Surf. Sci*. **1998**, *396*, 284.
(32) Li, S. Y.; Rodriguez, J. A.; Hrbek, J.; Huang, H. H.; Xu, G.-Q. *Surf. Sci.* **1996**, *366*, 29.
(33) Diez, R. P.; Jubert, A. H. *J. Mol. Catal*. **1992**, *73*, 65.
(34) Neurock, M.; van Santen, R. *J. Am. Chem. Soc*. **1994**, *116*, 4427.